Journal of Power Sources 230 (2013) 290–297

Contents lists available at SciVerse ScienceDirect

Journal of Power Sources

journal homepage: www.elsevier.com/locate/jpowsour

Composite membranes based on fully sulfonated poly(aryl ether ketone)/epoxy resin/different curing agents for direct methanol fuel cells

Tianyi Na [a], Ke Shao [a], Jing Zhu [a], Hongcheng Sun [a], Dan Xu [a], Zhuoqi Zhang [b], Christopher M. Lew [c], Gang Zhang [a,*]

[a] Alan G. MacDiarmid Institute, College of Chemistry, Jilin University, Changchun 130012, People's Republic of China
[b] School of Pharmaceutical Sciences, Jilin University, Changchun 130012, People's Republic of China
[c] Department of Chemical Engineering and Materials Science, University of Minnesota, Minneapolis, MN 55455, USA

HIGHLIGHTS

- Fully sulfonated side-chain-type polymer with was synthesized.
- Two composite membranes were obtained by introducing epoxy resin.
- The composite membranes had better selectivity and high proton conductivity.

ARTICLE INFO

Article history:
Received 11 June 2012
Received in revised form
22 November 2012
Accepted 13 December 2012
Available online 27 December 2012

Keywords:
Fuel cells
Polymer electrolyte membrane
Composite membranes
Epoxy resins

ABSTRACT

A fully sulfonated poly(aryl ether ketone) bearing pendent sulfoalkyl groups in the side chain (SNPAEK-100) is synthesized and used as the matrix membrane. Two series of composite membranes are obtained by introducing epoxy resins (TMBP) and two different curing agents with or without sulfonic acid groups (DDS and BDSA). All the membranes are investigated in detail as polymer electrolyte membranes. As expected, the water uptake, the methanol permeability, and the proton conductivity of the cross-linked membranes decrease with increasing epoxy resin content. Compared with STD-*x* membranes (0.101 S cm^{-1}–0.233 S cm^{-1}), the STB-*x* (0.171 S cm^{-1}–0.266 S cm^{-1}) membrane series reduce the loss of proton conductivity because of the sulfonated curing agent, BDSA. Other properties of the composite membranes, such as the mechanical properties and the thermal properties are also investigated. All the results indicate that the composite membranes based on SNPAEK-100 and BDSA are promising membrane candidates for direct methanol fuel cells.

1. Introduction

Polymer electrolyte membrane fuel cells (PEMFCs) are one of the promising energy sources because of their high power conversion and environmentally friendly system [1–3]. Among all kinds of fuel cell technologies, direct methanol fuel cells (DMFCs) with methanol as an energy source are one of the best candidates for portable applications [4]. Polymer electrolyte membrane (PEM) is considered to be the key component in the DMFCs. Currently, perfluorosulfonic acid (PFSA) polymer membranes, commonly known as Nafion (DuPont), have been widely used as the proton exchange membrane in DMFCs, due to their excellent chemical and thermal stability and high proton conductivity in the hydrated state [5]. However, several significant obstacles of Nafion have hampered their commercialization for DMFCs, such as high cost, high methanol permeability, and unstable proton conductivity at high temperature [6,7]. These limitations led to extensive research to modify the Nafion membrane [4,8]. However, improved results are achieved by either sacrificing the mechanical properties or increasing the membrane resistances.

Sulfonate-functionalized aromatic hydrocarbon polymers, such as sulfonated derivatives of poly(arylene ether ketone)s (SPAEK) [9], poly(arylene ether sulfone)s (SPAES) [2], and polyimides [10], have been studied extensively as alternative materials because their rigid, aromatic backbones confer high thermal stability, good mechanical strength, and reasonable chemical durability [11,12].

* Corresponding author. Tel./fax: +86 431 85168868.
E-mail address: gzhang@jlu.edu.cn (G. Zhang).

0378-7753/$ – see front matter © 2012 Elsevier B.V. All rights reserved.
http://dx.doi.org/10.1016/j.jpowsour.2012.12.082

However, the sulfonic acid groups located on the main chain and the rigid polyaromatic backbones prevent the continuous ion transport channels from forming distinct phase-separated structures [13].

One approach to enhance membrane performance is to induce hydrophilic–hydrophobic phase separated structures by positioning the sulfonic acid groups on side chains grafted onto the polymer main chains [14,15]. For example, Lee and co-workers reported segmented copoly(arylene ether sulfone) membranes having densely sulfonated pendent phenyl blocks, which showed high proton conductivities of 0.1–0.3 S cm^{-1} at 80 °C [15]. Also, Zhang et al. prepared cardo poly(aryl ether sulfone) copolymers bearing side chain pendent sulfoalkyl groups that had higher conductivity than the random polymers at the same ion-exchange capacity (IEC) level [16]. Generally, improved efforts are made by increasing the sulfonic acid group content, although a high degree of sulfonation induces high methanol permeability and excessive water swelling [17]. In previous work, we investigated a series of pendent polymers that showed comparable performance compared with Nafion membranes [18,19].

In the past few decades, many researchers attempted to apply composite doping or blending crosslinking technologies to modify the sulfonated poly(aryl ether ketone)s in order to improve the dimensional stabilities of the membranes and lower their methanol permeability at a high degree of sulfonation [20–22]. For example, epoxy resins exhibited strong performance and were widely used as composite materials in PEMs due to their two or more highly active epoxy groups, excellent stability, and electrical insulation [23,24]. Lee et al. mixed sulfonated polyimide with epoxy resins to prepare epoxy-based semi-interpenetrating polyimide networks [25]. The increasing amount of epoxy resin and crosslinking networks restricted the water absorption, improved the hydrolytic stability of sulfonated polyimide, and lowered the methanol permeability of composite membranes. Also, Fu et al. investigated a series of promising epoxy resins crosslinked with SPAEKs composite membranes [26,27]. These investigations also illustrated that this technology has excellent prospects for application as PEMs.

In this paper, we prepared a fully sulfonated poly(aryl ether ketone) bearing pendent sulfoalkyl groups in the side chain (SNPAEK-100), which is composited with epoxy resin. Furthermore, we prepared two series of composite systems by adding additional curing agents with or without sulfonic acid groups. The water uptake, proton conductivity, methanol permeability, and mechanical properties of the composite membranes were investigated as PEMs. All the results showed that mixing the epoxy resin and SPAEKs is a promising approach for preparing PEMs for DMFCs.

2. Experimental section

2.1. Materials

4,4′-diaminodiphenylsulfone (DDS), 2,2′-Benzidinedisulfonic acid (BDSA), and 4,4′-diglycidyl (3,3′,5,5′-tetramethylbiphenyl) epoxy resin (TMBP), were purchased from Sigma–Aldrich Ltd. Dimethyl sulfoxide (DMSO) and boron tribromide (BBr_3) (from Beijing Chemical Reagents) were vacuum-distilled before use. The monomer, 1,5-bis(4-fluorobenzoyl)-2,6-dimethoxy-naphthalene (DMNF), was obtained following the procedure in our previous study [28]. Other chemicals were purchased from Sigma–Aldrich and used without further purification.

2.2. Characterization

The ^1H NMR spectrum was measured on a 500 MHz Bruker Avance 510 spectrometer at 298 K with deuterated dimethyl sulfoxide (DMSO-d_6) as the solvent and tetramethylsilane (TMS) as the standard. The intrinsic viscosities of the polymers were measured at 0.5 g L^{-1} in DMF at 25 °C (±1) using an Ubbelodhe viscometer. The thermal stability was measured using a Pyris 1 TGA (Perkin–Elmer) system. All the membranes were heated from 100 °C to 700 °C at a heating rate of 10 °C min^{-1} in flowing nitrogen.

2.3. Synthesis of the fully sulfonated poly(aryl ether ketone) (SNPAEK-100) polymer

We chose fully sulfonated poly(aryl ether ketone) (SNPAEK-100) with a relative higher IEC (IEC = 2.30 meq g^{-1}) as the polymer matrix. It was synthesized and studied in our previous report [29] (Scheme 1). In brief, typical polycondensation reactions were first performed with calculated reactant amounts to ensure preparation of the fully sulfonated polymer. The two monomers (DMNF and BPA) were added at the same ratio (1:1) in the reaction. Then, demethylation reaction and sulfobutylation reaction were performed in order to obtain the polymers with –OH groups and SNPAEK-100 polymer, respectively.

2.4. Membrane preparation

The SNPAEK-100 was composited with 4,4′-diglycidyloxy-3,3′,5,5′-tetramethyl biphenyl (TMBP) and then cured with DDS and BDSA to form the composite membranes. Scheme 2 shows the synthesis procedure of the composite membranes. First, the SNPAEK-100 was dissolved in DMSO to form a 10 wt% solution. TMBP and DDS (or BDSA) were added to the solution to form a homogeneous mixture. The molar ratio of TMBP and DDS (or BDSA) was 2:1. Then, the resulting solutions were cast onto clean glass plates and dried at 60 °C for 24 h. Finally, the membranes underwent a curing procedure at 160 °C for 12 h and then 180 °C for 1 h. The membranes were removed from the glass plates and were immersed in a 1.0 M HCl solution overnight to obtain the membranes in acid form. The SNPAEK/TMBP/DDS (or SNPAEK/TMBP/BDSA) composite membranes were named STD-*x* (or STB-*x*), where *x* represented the mass fraction of TMBP/DDS (or TMBP/BDSA).

2.5. Water uptake and swelling ratio

The water uptake and swelling ratio of the membranes were measured as follows. The membranes were dried at 80 °C under vacuum for 12 h until a constant weight was obtained. Then, the dried membranes were immersed in deionized water at the desired temperature for 24 h. The membranes were taken out, wiped with tissue paper, and quickly measured for their weight and length (or thickness). Water uptake (WU) of the membranes was calculated from:

$$\text{water uptake}(\%) = \frac{W_{\text{wet}} - W_{\text{dry}}}{W_{\text{dry}}} \times 100\% \quad (1)$$

$$\text{swelling ratio}(\%) = \frac{T_{\text{wet}} - T_{\text{dry}}}{T_{\text{dry}}} \times 100\% \quad (2)$$

where W_{wet} and W_{dry} are the weight of the wet and dry membranes, respectively, and T_{wet} and T_{dry} are the length (or thickness) of the wet and dry membranes, respectively.

2.6. Ion-exchange capacity (IEC)

The IEC of the membranes was determined by a classical titration method. The membranes in acid form were immersed in

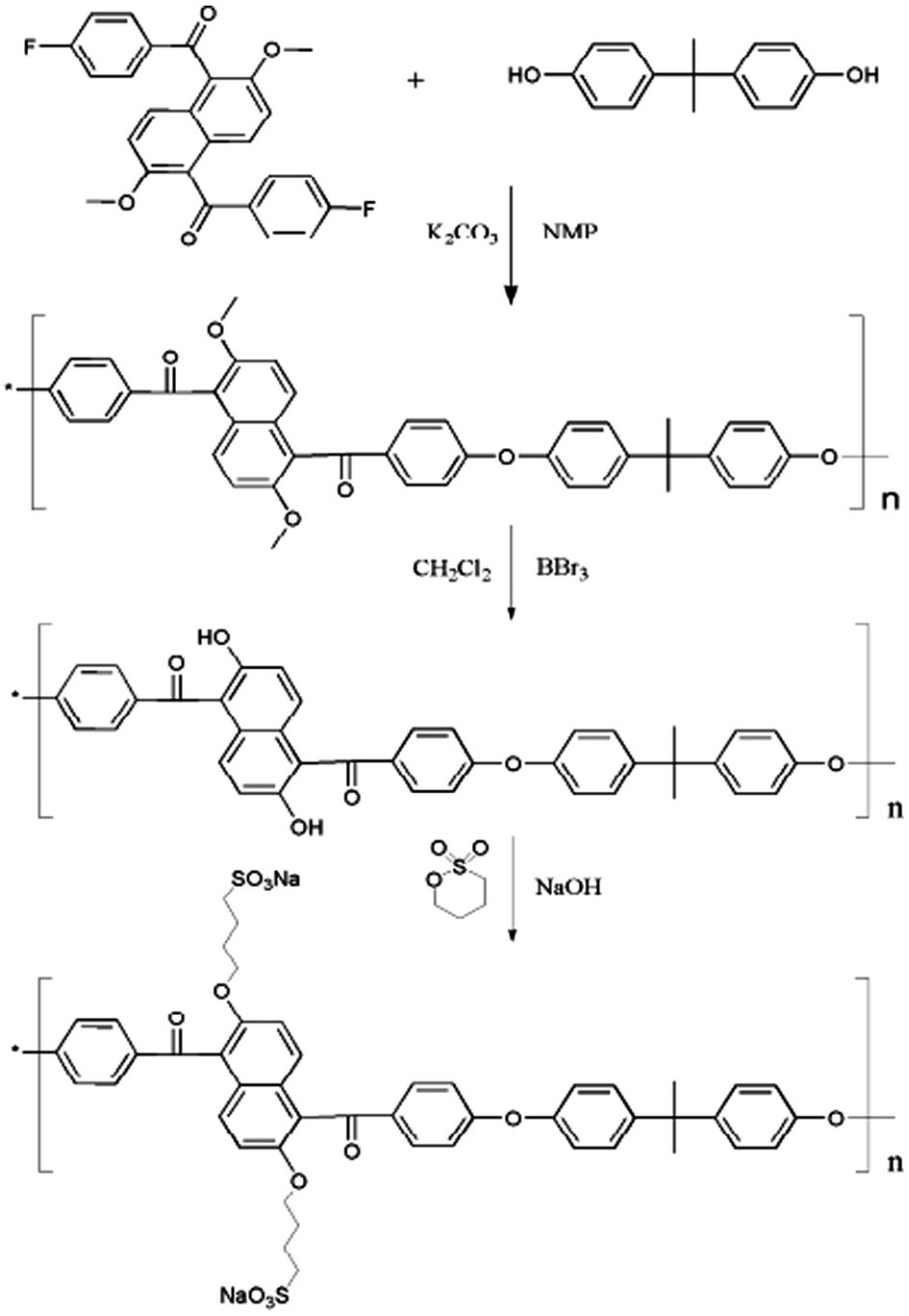

Scheme 1. The synthesis route of SNPAEK-100.

a 2 M sodium chloride solution for 48 h. The H^+ ions in solution were then titrated with 0.01 M sodium hydroxide using a phenolphthalein indicator. The IEC was calculated via the following relationship (3):

$$\mathrm{IEC} = \frac{\text{consumed ml NaOH} \times \text{molarity MaOH}}{\text{weight of dried membrane}} \left(\text{mequiv}\cdot\text{g}^{-1}\right) \tag{3}$$

2.7. Proton conductivity

Fully hydrated membranes (4 cm × 1 cm) were measured by a four-electrode AC impedance method from 0.1 Hz to 100 kHz, 10 mV AC perturbation, and 0.0 V DC rest voltage using a Princeton Applied Research Model 273A Potentiostat (Model 5210 frequency response detector, EG&G PARC, Princeton, NJ). The measurement was carried out with the cell immersed in constant-temperature water, and the proton conductivity was determined by the following equation [29]:

$$\sigma = \frac{L}{RA} \tag{4}$$

where σ is the proton conductivity, L is the distance between the electrodes used to measure the potential (L = 1 cm), R is the membrane resistance, and A is the membrane area.

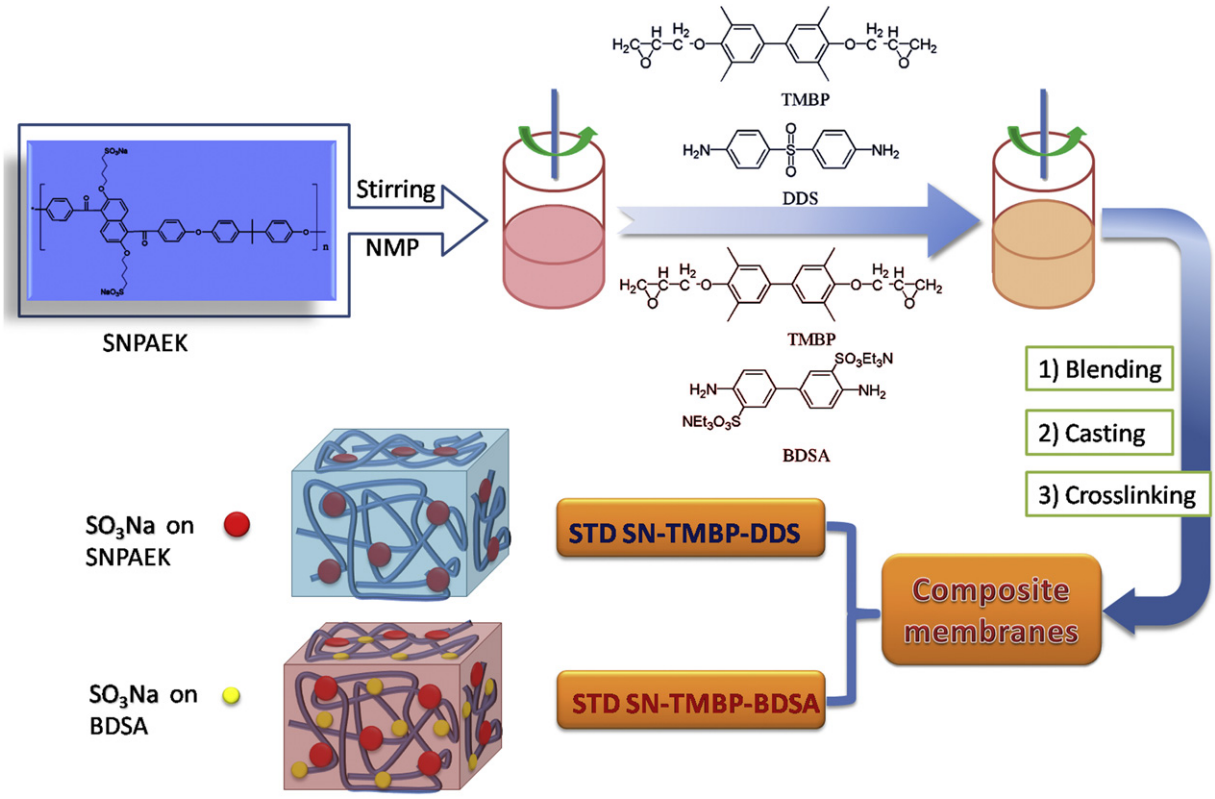

Scheme 2. Preparation of the composite membranes.

2.8. Methanol diffusion coefficient

A glass diffusion cell was used to measure the methanol permeability as described in the literature [29]. The cell consisted of two reservoirs that were separated by a membrane. A 10 M methanol solution and deionized water were placed on each side. Magnetic stirrers were used in each compartment to ensure uniformity. The concentration of the methanol in the water reservoir was determined by using a SHIMADZU GC-8A chromatograph. The methanol permeability was calculated as follows:

$$C_B(t) = \frac{A}{V_B}\frac{DK}{L}C_A(t - t_0) \quad (5)$$

where A (cm^2), L (cm), and V_B (mL) are the effective area, the thickness of the membranes, and the volume of the permeated reservoirs, respectively. C_A and C_B (mol m^{-3}) are the methanol concentrations in the feed and permeate, respectively. DK (cm^2 s^{-1}) denotes the methanol permeability.

2.9. Mechanical properties

The mechanical properties of the membranes were measured on a SHIMADZU AG-I 1KN. Membrane specimens (15 mm × 4 mm) were placed between the grips of the testing machine at a tensile rate of 2 mm min^{-1}. For each reported test, at least three measurements were taken and an average value was calculated.

3. Results and discussion

3.1. Synthesis and characterization of SNPAEK-100 and the composite membranes

Scheme 1 shows the synthetic route of SNPAEK-100. Fig. 1 shows ^{1}H NMR spectrum of SNPAEK-100. The peaks at H9 and H10, H11 and H8 were attributed to the sulfoalkyl groups. The signals between 6 ppm and 8 ppm were associated with the hydrogens of the aromatic rings. By comparing the area under the curve of the aromatic rings with that of H11, we calculated that 0.5n (sulfoalkyl)/n (repeat unit) = 0.97, which was very close to the theoretical value of 1.0. Fully sulfonated pendent polymers were prepared successfully.

The chemical structures of the composite membranes were confirmed by FT-IR spectroscopy. Fig. 2(a) and (b) shows the FTIR of

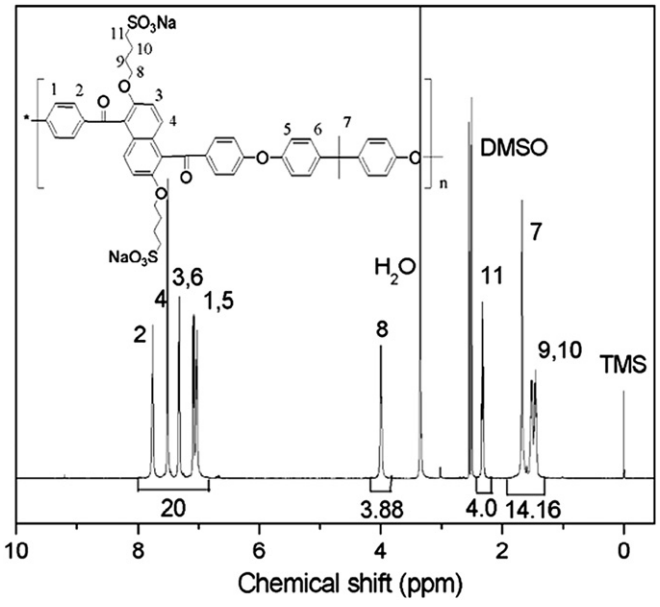

Fig. 1. ^{1}H NMR spectrum of SNPAEK-100.

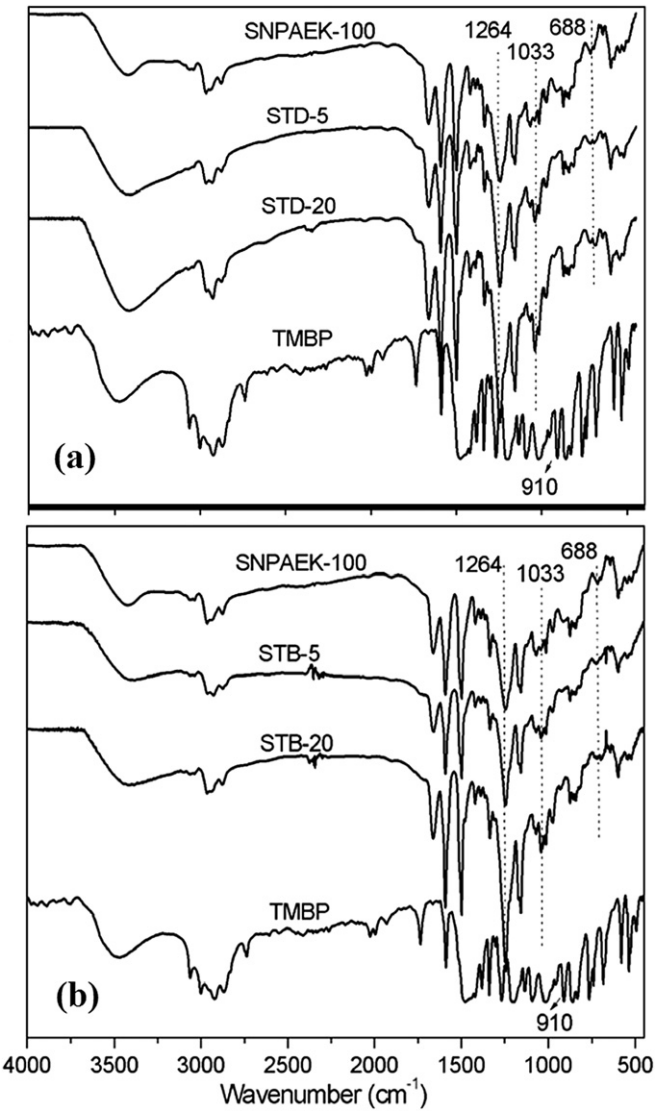

Fig. 2. FTIR spectra of the membranes. (a) SNPAEK-100 membranes and STD-*x* membranes. (b) SNPAEK-100 membranes and STB-*x* membranes.

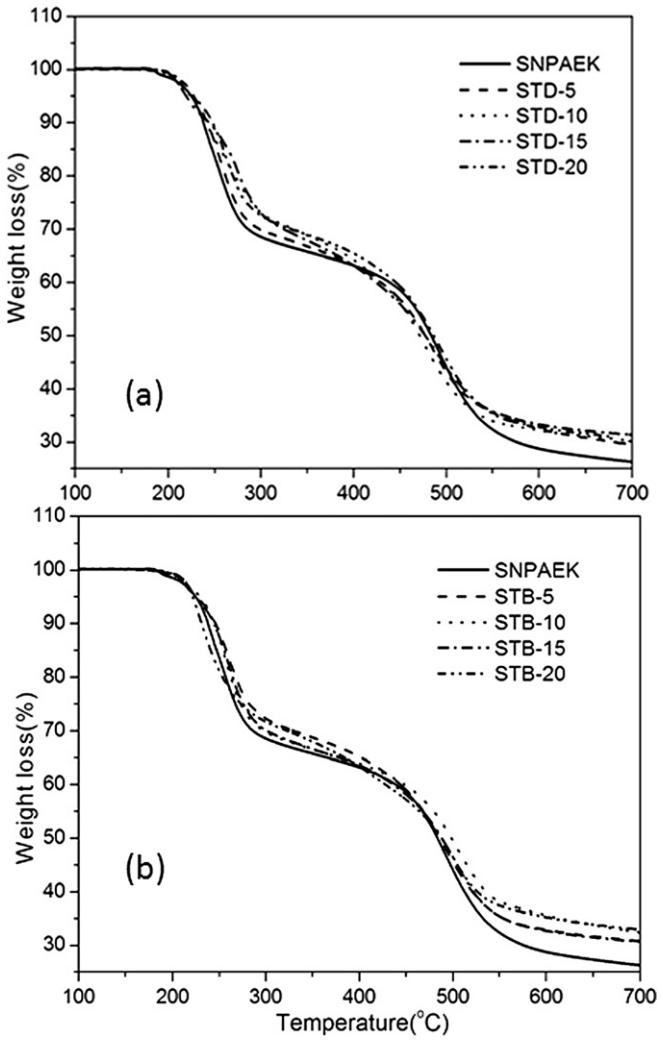

Fig. 3. TGA curves of the composite membranes. (a) SNPAEK-100 membranes and STD-*x* membranes. (b) SNPAEK-100 membranes and STB-*x* membranes.

STD-*x* membranes and STB-*x* membranes, respectively. The FTIR of SNPAEK-100 membranes and TMBP were also included. The absorption bands at 1033 and 1264 cm^{-1} can be assigned to asymmetric and symmetric O═S═O stretching vibrations of sulfonate groups. The absorption band at 688 cm^{-1} can be assigned to the S—O stretching of sodium sulfonate groups. As can be seen from Fig. 2, the STD-*x* composite membrane retains all the absorption peak of sulfonic acid. And the absorption band at 910 cm^{-1}, which is assigned to epoxy group, could not be found. This result illustrated the epoxy resin in the composite membrane cured completely.

3.2. Thermal properties of the membranes

The thermal stability of the polymers was evaluated by TGA analysis. Fig. 3 shows the curves of the two different composite membranes. Fig. 3(a) shows the stability of STD-*x* membranes and SNPAEK-100 membranes. From the curves, we can see that the original SNPAEK-100 membrane showed excellent thermal stability and the temperature for 5% weight loss was observed over 200 °C. Also, a two-step weight loss was observed for the composite membranes and the pure SNPAEK-100 membrane at 190 °C—300 °C and 450 °C to 580 °C. The first weight loss observed from 190 °C to 300 °C was attributed to the decomposition of the pendent sulfonic

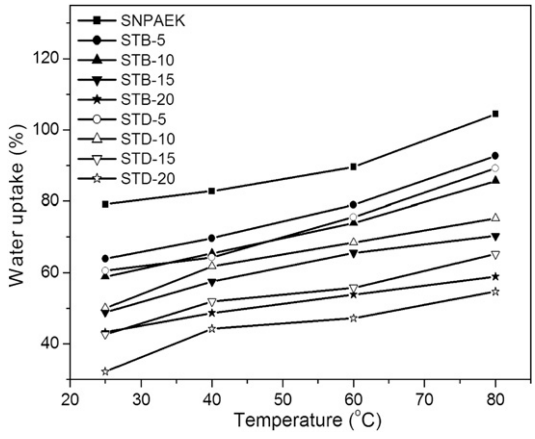

Fig. 4. Water uptake of the composite membranes as a function of temperature.

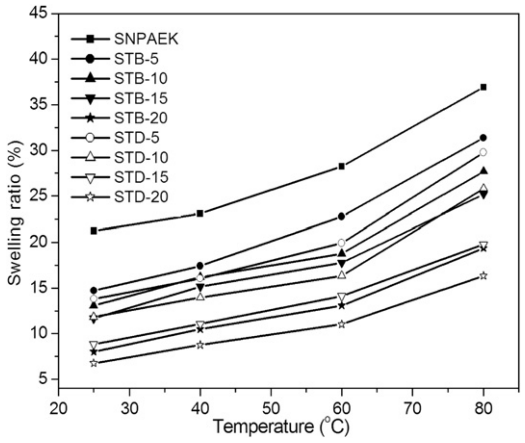

Fig. 5. Swelling ratio of the composite membranes as a function of temperature.

acid groups. The second decomposition stage from 450 °C to 580 °C was assigned to the degradation of the main and side chains [30]. Because the thermal stability of TMBP and DDS are better than SNPAEK, the thermal curing reaction made the membrane more compact and the composite membranes showed better thermal stability then the pure membrane. Fig. 3(b) shows that the STB-*x* membranes have similar thermal properties as the STD-x membranes.

3.3. Water uptake and swelling ratio

The water uptake and swelling ratio are very important properties for PEMs because the protons need water in order to pass through the PEMs in the form of H_3O^+ and $H_5O_2^+$. However, higher water uptake usually results in the reduction in the dimensional stability of PEMs, which causes a loss in the mechanical properties and the decline of methanol resistance. A lower water uptake and swelling ratio are required for PEMs. Figs. 4 and 5, and Table 1 show the water uptake and swelling ratio of all the membranes. The SNPAEK-100 membrane showed high water uptake of 104.4% and a swelling ratio of 36.9% at 80 °C. Considering the fully sulfonated condition, the water uptakes were lower than the main-chain type polymers at the same degree of sulfonation. Both of the two composite membrane systems showed lower water uptake and swelling ratios than those of the pristine membrane. STD-20 showed the lowest water uptake (54.7%) and swelling ratio (16.3%). All the STB-*x* membranes showed a little higher water uptake than the STD-*x* membranes, which may be due to the sulfonic acid groups in the membranes. The dimensional stability may result from the cross-linking epoxy resin, which compact the structure of the membranes. The cross-linking reaction could effectively limit the motion of the polymer chains, leading to better dimensional stability than the SNPAEK-100 membrane.

3.4. Ion-exchange capacity (IEC)

The IEC value has a close relationship with the proton conductivity and water uptake and is an important property that indicates the quantity of exchangeable protons in the membranes [31]. Table 1 lists the IEC values of the composite membranes and the pristine membrane. Since introducing the epoxy resins diluted the ion concentration in the polymer membranes, the IEC values decreased with increasing content of the two epoxy resins. However, the IEC values of STB-*x* membranes were higher than the STD-*x* membranes at the same content of the epoxy resin, which may be due to the sulfonic acid groups in BDSA.

3.5. Proton conductivity, methanol diffusion coefficient, and selectivity

The proton conductivity was measured by a four-electrode ac impedance method. The proton conductivity values of the composite membranes were compared to the pristine SNPAEK-100 membrane. Fig. 6 shows the proton conductivities of the membranes plotted against temperature. Usually, the proton conductivity is considered the most important property in the evaluation of PEMs. The proton conductivities of all the membranes followed the same trends as the IEC values and increased with temperature; in other words, as the IEC increased, the proton conductivity was also higher. At 80 °C, most of the proton conductivities of the membranes were higher than 0.1 S cm^{-1}, which is the minimum requirement in practical applications. The SNPAEK-100 was fully sulfonated and provided enough proton conductivity polymer matrix. The side-chain-type polymer is composed of continuous ion-conducting pathways, which increases the proton conductivity of the membranes. The lower proton conductivity of STD-20 may be caused by an excessive concentration of epoxy resin, which diluted the amount of sulfonic acid groups in the composite membranes. Because the epoxy resins and curing agents in the composite membranes reduced the relative amount of the sulfonic acid groups, the proton conductivity of SNPAEK-100 was higher than all the composite membranes over the whole range of temperatures. Meanwhile, the proton conductivities of the STB-x membranes were all higher than the STD-*x* membranes at the same content of the epoxy resins. At 80 °C, the proton conductivity of STB-15

Table 1
The properties of STD-*x* and STB-*x* composite membranes.

Composite membranes	d[a] (μm)	IEC (meq g^{-1})	Water uptake (%)		Swelling ratio (%)		Methanol diffusion coefficient (× 10^{-7} cm^2 s^{-1})	Proton conductivity (S cm^{-1})	
			25 °C	80 °C	25 °C	80 °C		25 °C	80 °C
SNPAEK-100	68	2.30	79.2	104.4	21.2	36.9	17.2	0.123	0.270
STD-5	91	2.16	60.6	89.2	13.8	29.8	8.59	0.099	0.233
STD-10	73	1.91	50.1	75.2	11.8	25.8	6.03	0.080	0.191
STD-15	105	1.67	42.7	65.2	8.8	19.8	3.65	0.064	0.139
STD-20	59	1.52	32.2	54.7	6.8	16.3	2.81	0.059	0.101
STB-5	53	2.21	63.9	92.7	14.7	31.4	10.7	0.105	0.266
STB-10	86	2.07	58.9	85.7	13.1	27.7	7.63	0.090	0.253
STB-15	63	1.97	48.9	70.3	11.7	25.2	5.21	0.087	0.221
STB-20	95	1.74	43.3	58.9	8.0	19.4	3.59	0.070	0.171
Nafion	–	0.90	19.0	28.6	–	–	15.5	0.057	0.125

[a] Thickness of membranes.

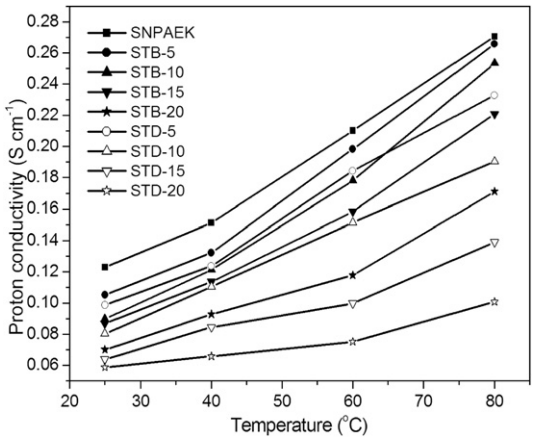

Fig. 6. Proton conductivity of the composite membranes.

(0.221 S cm^{-1}) and STB-5 (0.266 S cm^{-1}) were almost the same as the pristine SNPAEK-100 membrane (0.270 S cm^{-1}). This result shows that the sulfonated curing agent, BDSA, can effectively reduce the loss of proton conductivity in the composite film.

The proton conduction and methanol permeation take place through the same hydrophilic cluster channels in PEMs. The PEMs must provide both high proton conductivity and high methanol resistance [32]. Like fully sulfonated SNPAEK-100, polymers with a high degree of sulfonation usually exhibit higher methanol permeability [29]. Table 1 lists the methanol diffusion coefficients of the composite membranes and the pristine membrane. Compared to the SNPAEK-100 membrane (17.2×10^{-7} cm^2 s^{-1}), the methanol permeabilities of the composite membranes were much lower ($2.81–10.7 \times 10^{-7}$ cm^2 s^{-1}). The crosslinked network structure in the composite membranes limits movement between the polymer chains, and increases the resistance to methanol permeability. The methanol permeability of the composite membranes significantly decreased with higher epoxy resin concentrations. However, for the STB-*x* membranes, the methanol permeability was higher than the STD-*x* membranes due to the sulfonic acid within the cross-linked network.

The selectivity, which is the ratio of proton conductivity to methanol permeability, is the all-around factor in the evaluation of the membrane performance for DMFC applications [33]. Fig. 7 shows the selectivity of the two series of cross-linked membranes and the pristine membrane. As seen, the selectivity increased with the epoxy resin content. All the cross-linked membranes showed higher selectivity than SNPAEK-100. Compared with the SNPAEK-100 membrane, although the cross-linked membranes showed a little lower proton conductivity, they could still be used in DMFCs because of their low methanol permeability and higher selectivity.

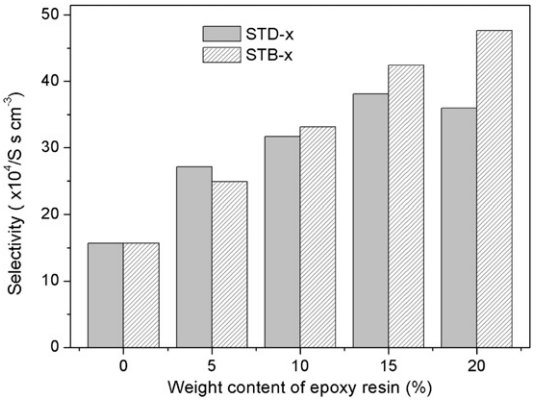

Fig. 7. Selectivity of the composite membranes.

Table 2
The mechanical properties of the STD-*x* and STB-*x* composite membranes.

Composite membranes	Tensile strength (MPa)	Young's Modulus (MPa)	Elongation at break (%)
SNPAEK-100	37.25	946.86	11.32
STD-5	40.13	1074.83	18.12
STD-10	41.58	1089.12	20.08
STD-15	39.43	1036.82	12.76
STD-20	33.01	779.49	4.32
STB-5	40.58	1027.45	10.64
STB-10	39.75	1014.82	15.06
STB-15	44.75	1416.63	18.84
STB-20	48.85	1396.07	14.96
Nafion	38.00	180	301.50

3.6. Mechanical properties of polymer membranes

Table 2 lists the mechanical properties of all the composite membranes and the pure SNPAEK-100 membrane tested in the dry state. Most of the composite membranes showed that the introduction of epoxy resin to the polymer matrix improved the mechanical properties of the composite membrane. In the composite membrane, the cross-linked network reduced the free volume of the system and restricted the molecular motion of the polymer chains of SNPAEK-100, and thus improved the mechanical properties of the membranes [24]. The STD-20 membrane showed a reduction in the mechanical properties, which may be caused by the poor compatibility between epoxy resin and SNPAEK-100. However, STB-10 showed a different result: the sulfonic acid groups in the BDSA may improve the compatibility. Thus, the mechanical properties still increased when the TMBP/BDSA content was higher than 10%. STB-15 had the best mechanical properties with a tensile strength of 44.75 MPa, a Young's modulus of 1416.63 MPa, and the elongation at break at 18.84%. The introduction of BDSA into the membranes is the key for improving the mechanical properties.

4. Conclusions

We have reported the preparation and comparison of two series of composite membranes based on sulfonated side-chain-type poly(aryl ether ketone) and two different epoxy resins. The SNPAEK was fully sulfonated to allow a polymer matrix with high proton conductivity. Two different epoxy resins were introduced with and without sulfonic acid groups. The composite membranes were investigated and compared with the pristine membrane as PEMs in DMFCs. The crosslinking network structures in the composite membranes compact the membrane and increased the density of sulfonic acid groups. As a result, the water uptake, swelling ratio, methanol permeability, and proton conductivity of the composite membranes were lower than those of the pristine membrane. The proton conductivities of the STB-*x* membranes were higher than those of the STD-*x* membranes. The selectivity of the membranes indicated that the STB-*x* membranes were a promising choice as PEMs. Future investigations will focus on the impact of the epoxy resin structure on the membranes.

Acknowledgments

This work was supported by the National Natural Science Foundation of China (Grant No. 21074044 & 51101073) and the Special Fund for Basic Scientific Research of Central Colleges, Jilin

University (No. 201103088) and Doctoral Program of Higher Education of China (No. 20110061120019).

References

[1] C.Y. Wang, Chem. Rev. 104 (2004) 4727–4766.
[2] T. Nakagawa, K. Nakabayashi, T. Higashihara, M. Ueda, J. Mater. Chem. 20 (2010) 6662–6667.
[3] B.C.H. Steele, A. Heinzel, Nature 414 (2001) 345–352.
[4] S.K. Nataraj, C.H. Wang, H.C. Huang, H.Y. Du, S.F. Wang, Y.C. Chen, L.C. Chen, K.H. Chen, ChemSusChem 5 (2012) 392–395.
[5] T. Li, G.M. Zhong, R.Q. Fu, Y. Yang, J. Membr. Sci. 354 (2010) 189–197.
[6] Y. Chang, G.F. Brunello, J. Fuller, M. Hawley, Y.S. Kim, M.D. Miller, M.A. Hickner, S.S. Jang, C. Bae, Macromolecules 44 (2011) 8458–8469.
[7] N. Zhang, G. Zhang, D. Xu, C.J. Zhao, W.J. Ma, H.T. Li, Y. Zhang, S. Xu, H. Jiang, H.C. Sun, H. Na, Int. J. Hydrogen Energy 36 (2011) 11025–11033.
[8] H.D. Lin, C.J. Zhao, W.J. Ma, H.T. Li, H. Na, J. Membr. Sci. 345 (2009) 242–248.
[9] H. Hu, M. Xiao, S.J. Wang, Y.Z. Meng, Int. J. Hydrogen Energy 35 (2010) 682–689.
[10] K. Miyatake, H. Zhou, T. Matsuo, H. Uchida, M. Watanabe, Macromolecules 37 (2004) 4961–4966.
[11] K. Xu, H. Oh, M.A. Hickner, Q. Wang, Macromolecules 44 (2011) 4605–4609.
[12] Y.H. Seong, J. Won, S.K. Kim, K. Nam, S.K. Kim, D.W. Kim, Int. J. Hydrogen Energy 36 (2011) 8492–8498.
[13] C.Y. Wang, N.W. Li, D.W. Shin, S.Y. Lee, N.R. Kang, Y.M. Lee, et al., Macromolecules 44 (2011) 7296–7306.
[14] N. Li, D.W. Shin, D.S. Hwang, Y.M. Lee, M.D. Guiver, Macromolecules 43 (2010) 9810–9820.
[15] N. Li, D.S. Hwang, S.Y. Lee, Y.L. Liu, Y.M. Lee, M.D. Guiver, Macromolecules 44 (2011) 4901–4910.
[16] Q.A. Zhang, F.X. Gong, S.B. Zhang, S.H. Li, J. Membr. Sci. 367 (2011) 166–173.
[17] M.M. Han, G. Zhang, K. Shao, H.T. Li, Y. Zhang, M.Y. Li, et al., J. Mater. Chem. 20 (2010) 3246–3252.
[18] Y. Zhang, Y. Wan, C.J. Zhao, K. Shao, G. Zhang, H.T. Li, et al., Polymer 50 (2009) 4471–4478.
[19] Y. Zhang, G. Zhang, Y. Wan, C.J. Zhao, K. Shao, H.T. Li, et al., J. Polym. Sci. Part A Polym. Chem. 48 (2010) 5824–5832.
[20] S.D. Mikhailenko, K. Wang, S. Kaliaguine, et al., J. Membr. Sci. 233 (2004) 93–99.
[21] S.P. Nunes, B. Ruffmann, E. Rikowski, et al., J. Membr. Sci. 203 (2002) 215–225.
[22] S.M.J. Zaidi, S.D. Mikhailenko, G.P. Robertson, et al., J. Membr. Sci. 173 (2000) 17–34.
[23] S. Wang, G. Zhang, M.M. Han, H.T. Li, Y. Zhang, J. Ni, et al., Int. J. Hydrogen Energy 36 (2011) 8412–8421.
[24] M.M. Han, G. Zhang, M.Y. Li, S. Wang, Z.G. Liu, H.T. Li, et al., J. Power Sources 196 (2011) 9916–9923.
[25] C.H. Lee, Y.Z. Wang, J. Polym. Sci. Part. A Polym. Chem. 46 (2008) 2262–2276.
[26] T.Z. Fu, S.L. Zhong, Z.M. Cui, C.J. Zhao, et al., J. Appl. Polym. Sci. 111 (2009) 1335–1343.
[27] T.Z. Fu, C.J. Zhao, S.L. Zhong, G. Zhang, K. Shao, et al., J. Power Sources 165 (2007) 708–716.
[28] K. Shao, J. Zhu, C.J. Zhao, X.F. Li, Z.M. Cui, Y. Zhang, et al., J. Polym. Sci. Part A Polym. Chem. 47 (2009) 5772–5783.
[29] J. Zhu, K. Shao, G. Zhang, C.J. Zhao, Y. Zhang, H.T. Li, et al., Polymer 51 (2010) 3047–3053.
[30] A. Collier, H.J. Wang, X.Z. Yuan, J.J. Zhang, D.P. Wilkinson, Int. J. Hydrogen Energy 31 (2006) 1838–1854.
[31] J.Y. Park, T.H. Kim, H.J. Kim, J.H. Choi, Y.T. Hong, Int. J. Hydrogen Energy 37 (2012) 2603–2613.
[32] H.W. Zhang, H.P. Huang, P.K. Shen, Int. J. Hydrogen Energy 37 (2012) 6875–6879.
[33] H. Ahmad, S.K. Kamarudin, U.A. Hasran, W.R.W. Daud, Int. J. Hydrogen Energy 35 (2010) 2160–2175.